

Experimental Study of Photodisintegration Cross Sections on ${}^3\text{He}$ and ${}^4\text{He}$ at Low Energies

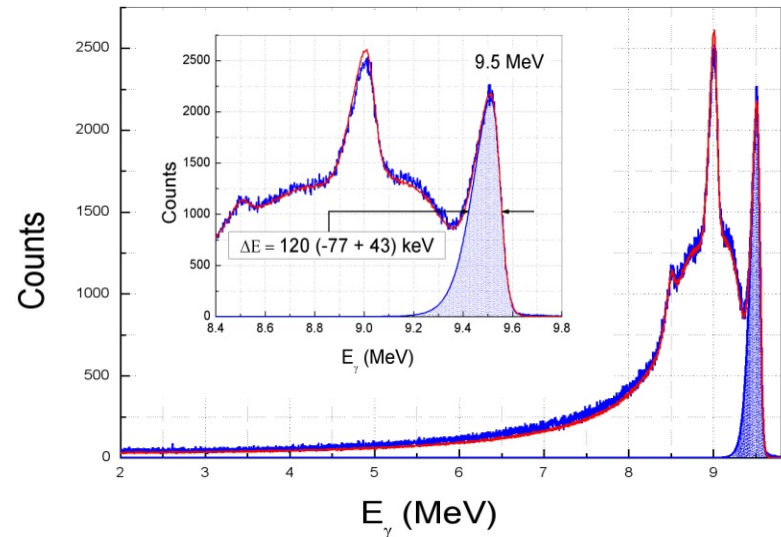
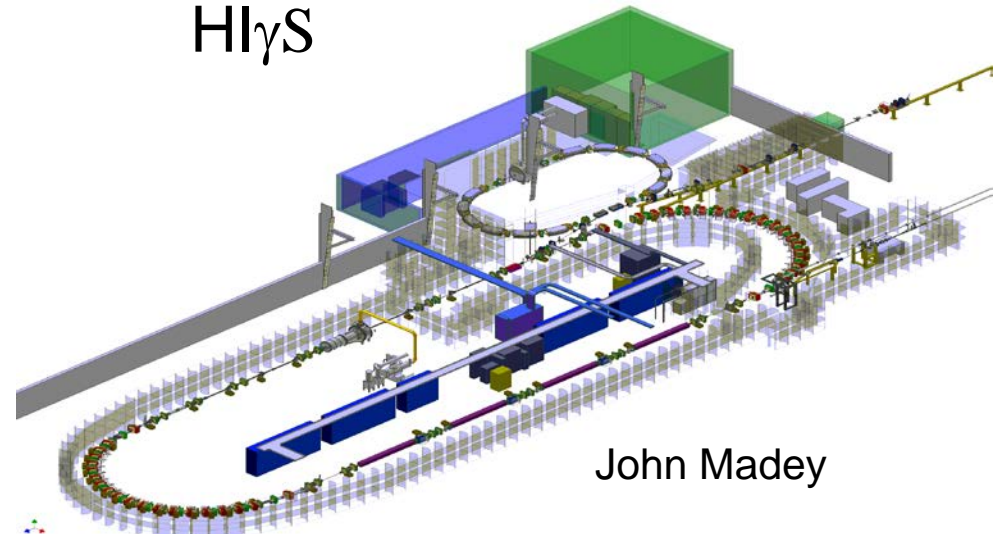
Werner Tornow

Duke University & Triangle Universities Nuclear Laboratory

Outline

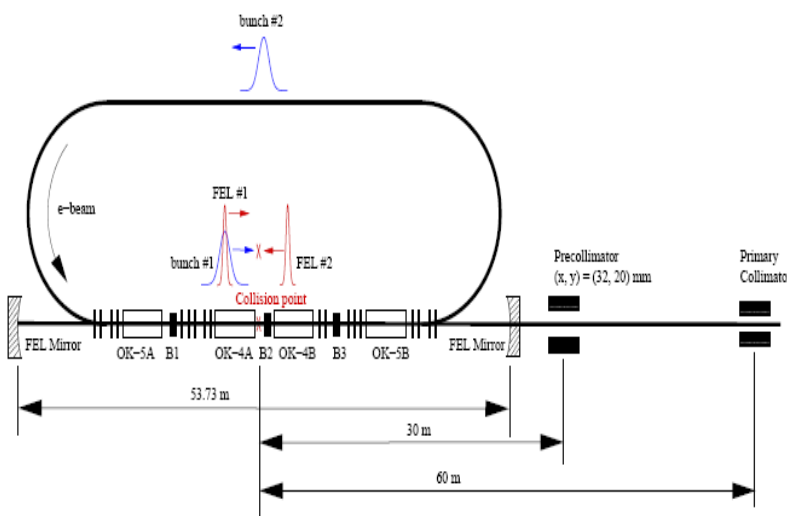
- ${}^3\text{He}(\gamma, \text{pd}) \sigma_{\text{tot}}$ between $E_\gamma = 7$ and 16 MeV
- ${}^4\text{He}(\gamma, \text{pt}) \sigma_{\text{tot}}$ between $E_\gamma = 22$ and 29.5 MeV
- ${}^4\text{He}(\gamma, {}^3\text{He})n \sigma_{\text{tot}}$ between $E_\gamma = 27 - 28$ MeV
- ${}^3\text{He}(n, n){}^3\text{He}$ $A_y(\theta)$ between $E_n = 1.6$ and 5.4 MeV

H_I γ S



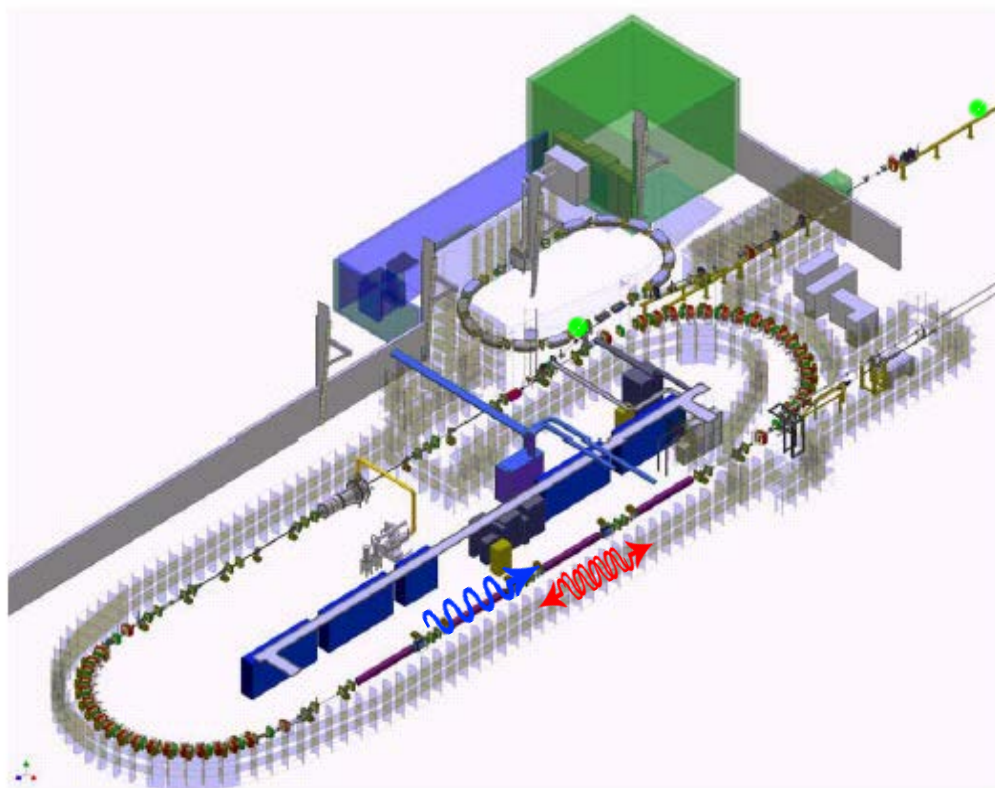
Quasi monoenergetic
 γ -ray flux on target: $>10^8 s^{-1}$

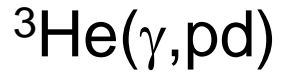
Tunable from 1 to 97 MeV
100% linear or circular polarization
Energy resolution determined by
Collimation; no need for tagging



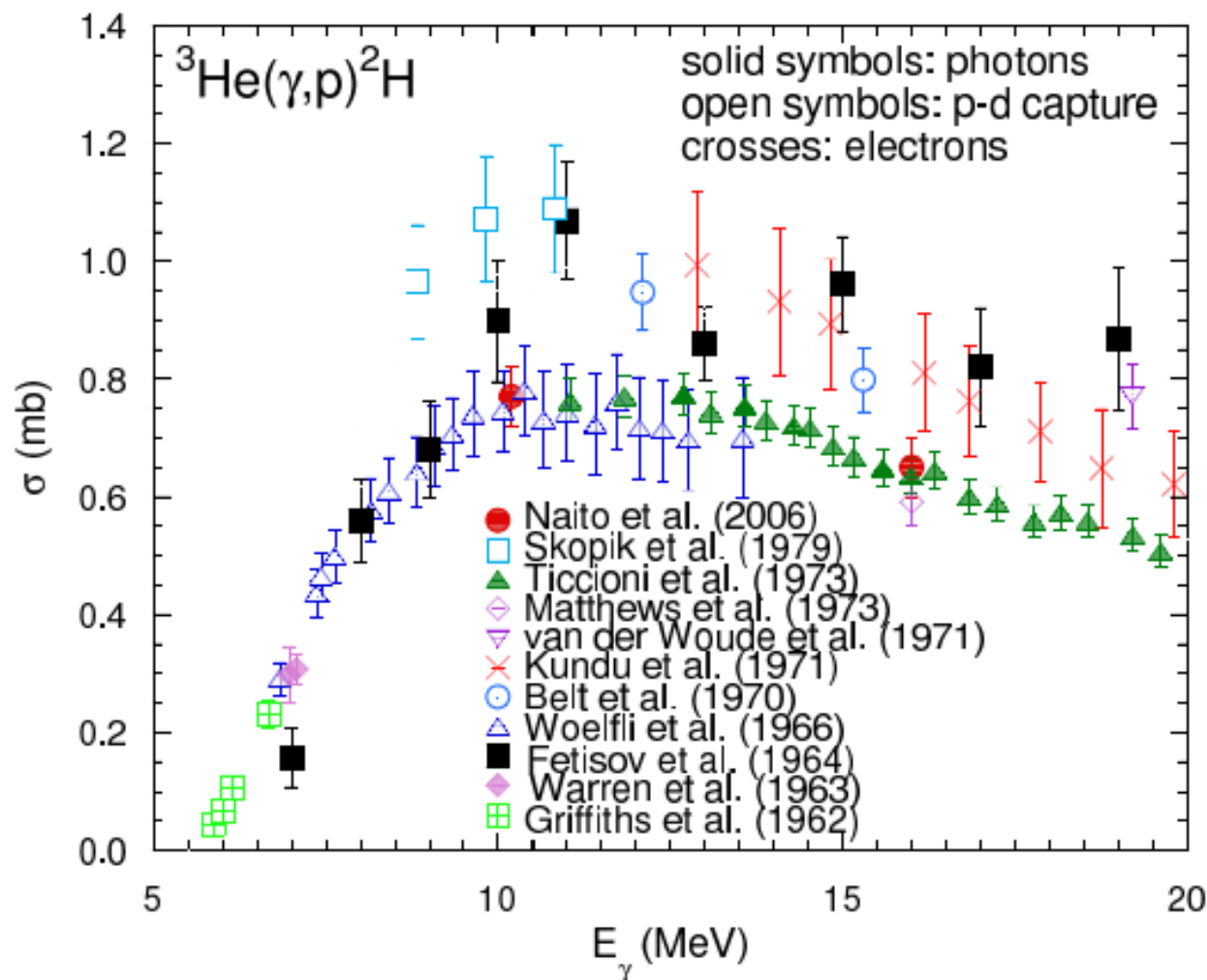
Vladimir Litvinenko (1992)

HI γ S Facility at TUNL

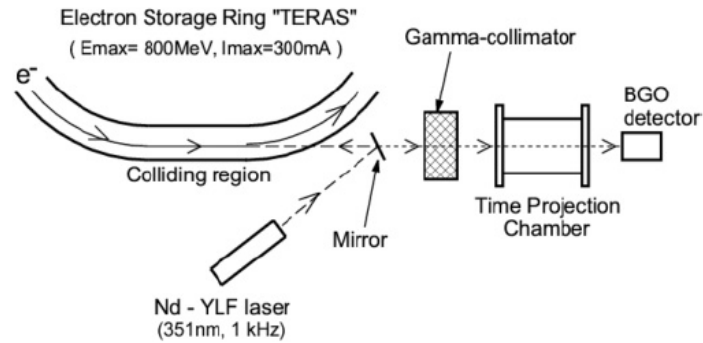




Q=-5.49 MeV



National Institute of Advanced Industrial Science and Technology (AIST)
Tsukuba, Japan



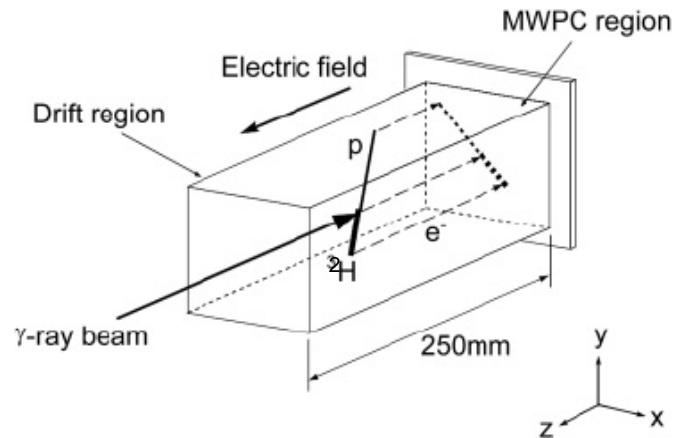
$\sim 1.7 \text{ MeV } \gamma\text{-ray energy width}$

$10^4 \gamma$ rays per second

Shima *et al.*, 2005

Time projection chamber

as target as detector



We don't have a time-projection chamber

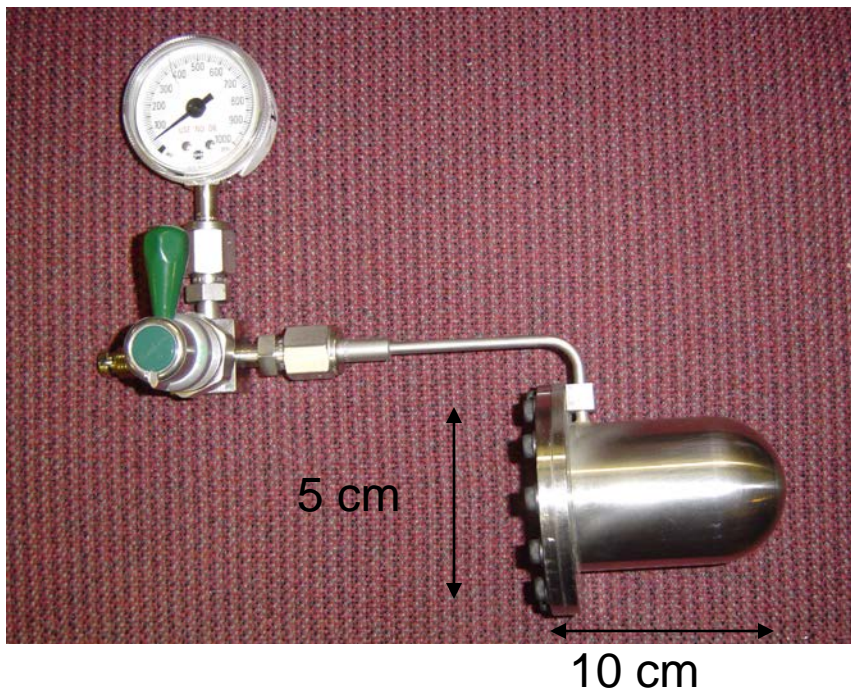
We used ${}^3\text{He}$ -Xe high-pressure gas scintillators instead

Xe admixture ($\sim 5 - 10\%$) is needed :

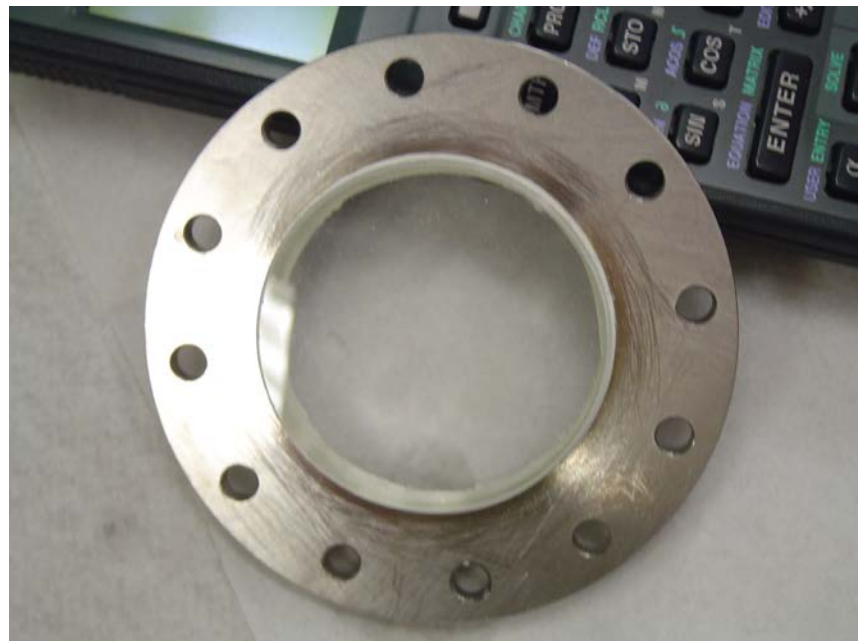
- a) to increase light output, *i.e.*, energy resolution
- b) provide stopping power for the protons within scintillator volume (proton energies vary from 1.1 MeV at $E_\gamma = 7$ MeV to 7.6 MeV at $E_\gamma = 16$ MeV)

Construction

1 mm thick stainless steel



1 cm thick glass window

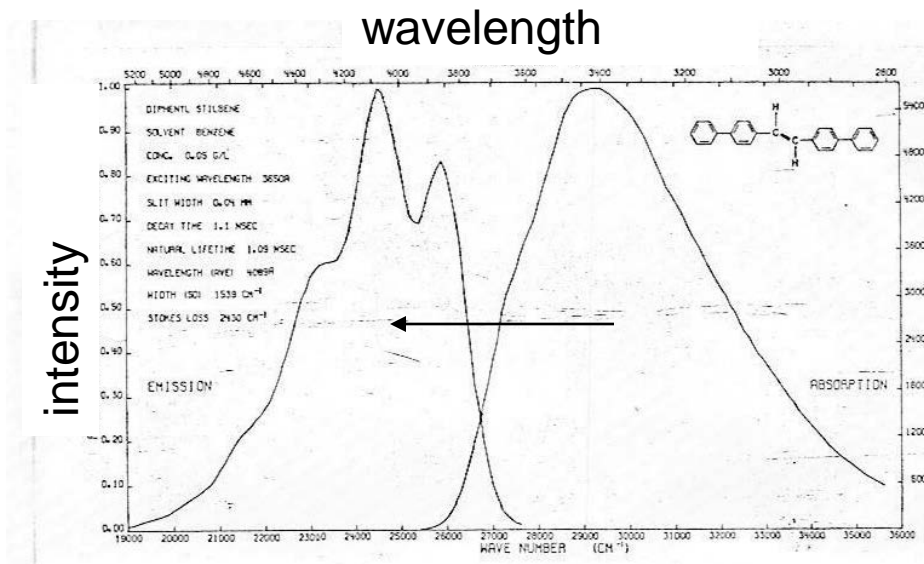


Glue Maxos glass window into cap
Araldit + Hardener

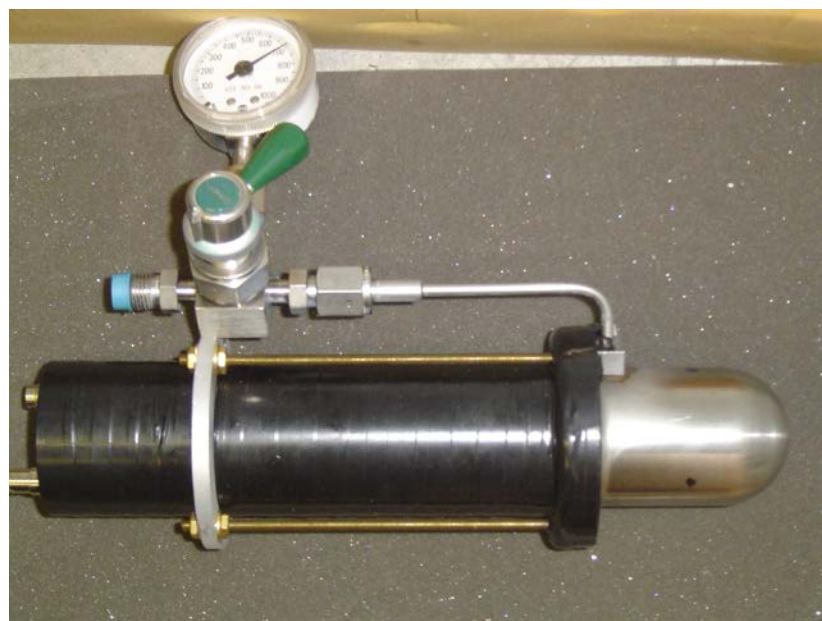
- MgO creates white film on gas cell walls



- Evaporate Diphenylstilbene (DPS) onto glass window and inside of gas cell
- DPS shifts the wavelength from 340 nm to 410 nm



- Fill cell with ${}^3\text{He}$ (95%) and Xenon (5%)
 - (Xenon is also a wavelength shifter)
- Attach PMT to gas cell

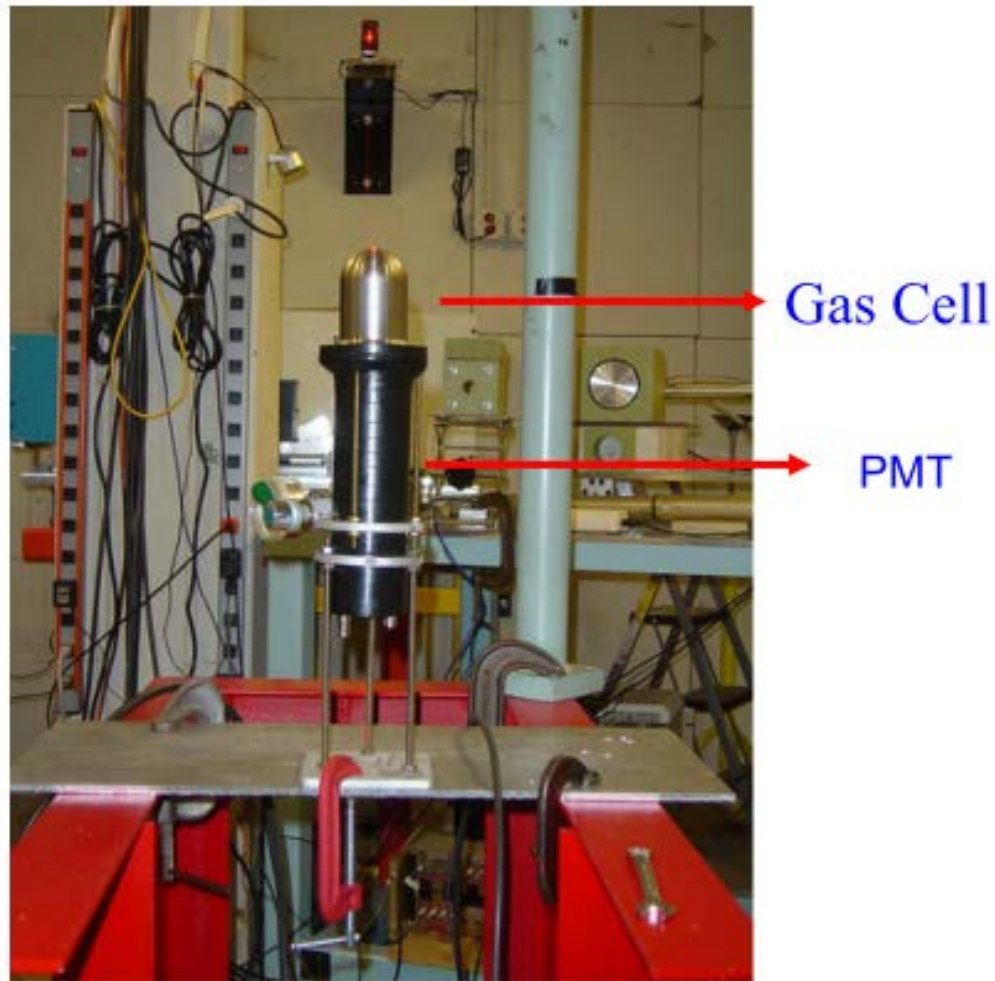


- Pressure test cell bringing pressure to 1000 psi



- Response function is linear
- Light output is independent of particle type
- Energy resolution is energy dependent
- ${}^3\text{He-Xe}$ gas scintillators have very good energy resolution (2-10%)

Experimental Setup



^3He and Xe pressures used for $^3\text{He}(\gamma, \text{pd})$ experiment

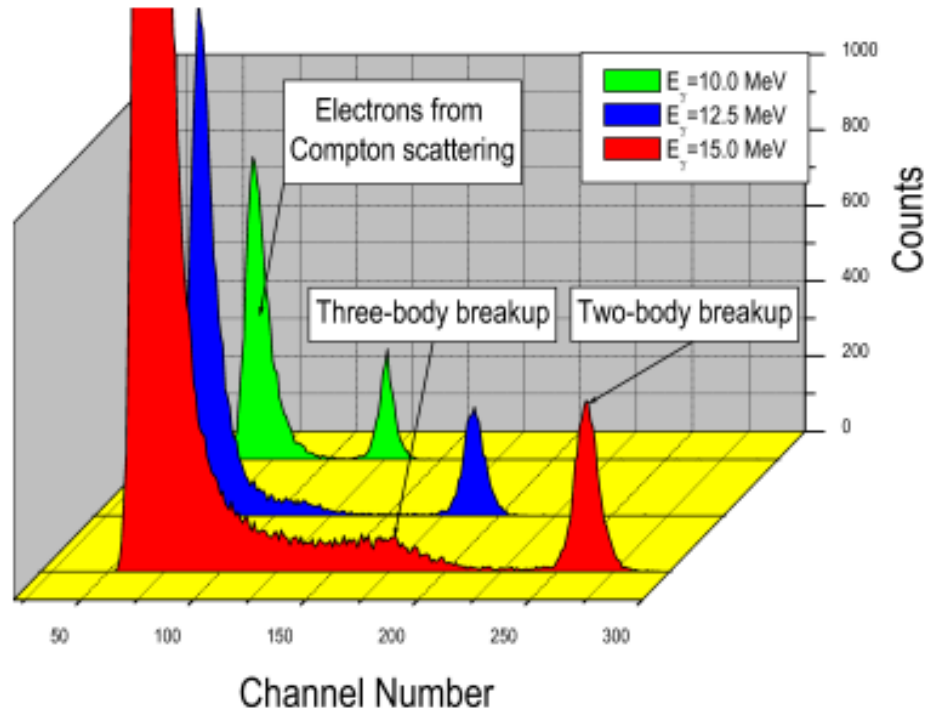
42 psi Xe & 458 psi ^3He at 6.96 and 7.93 MeV

148 psi Xe & 602 psi ^3He at 8.78, 9.85, 10.85 12.78 MeV

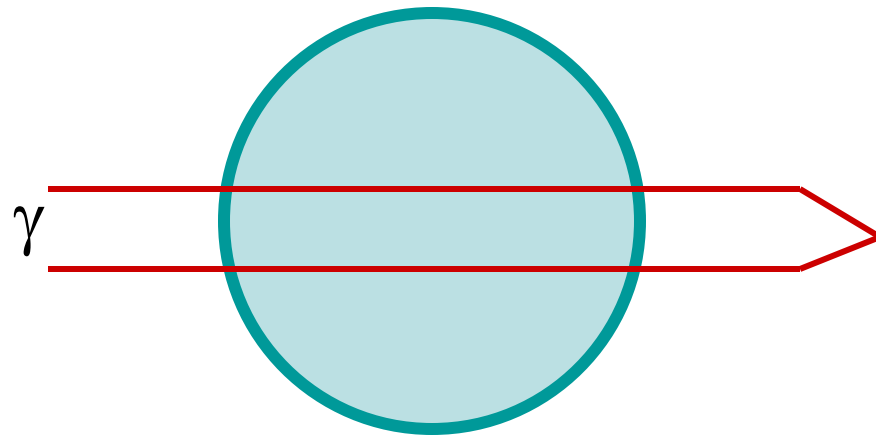
132 psi Xe & 528 psi ^3He at 12 MeV

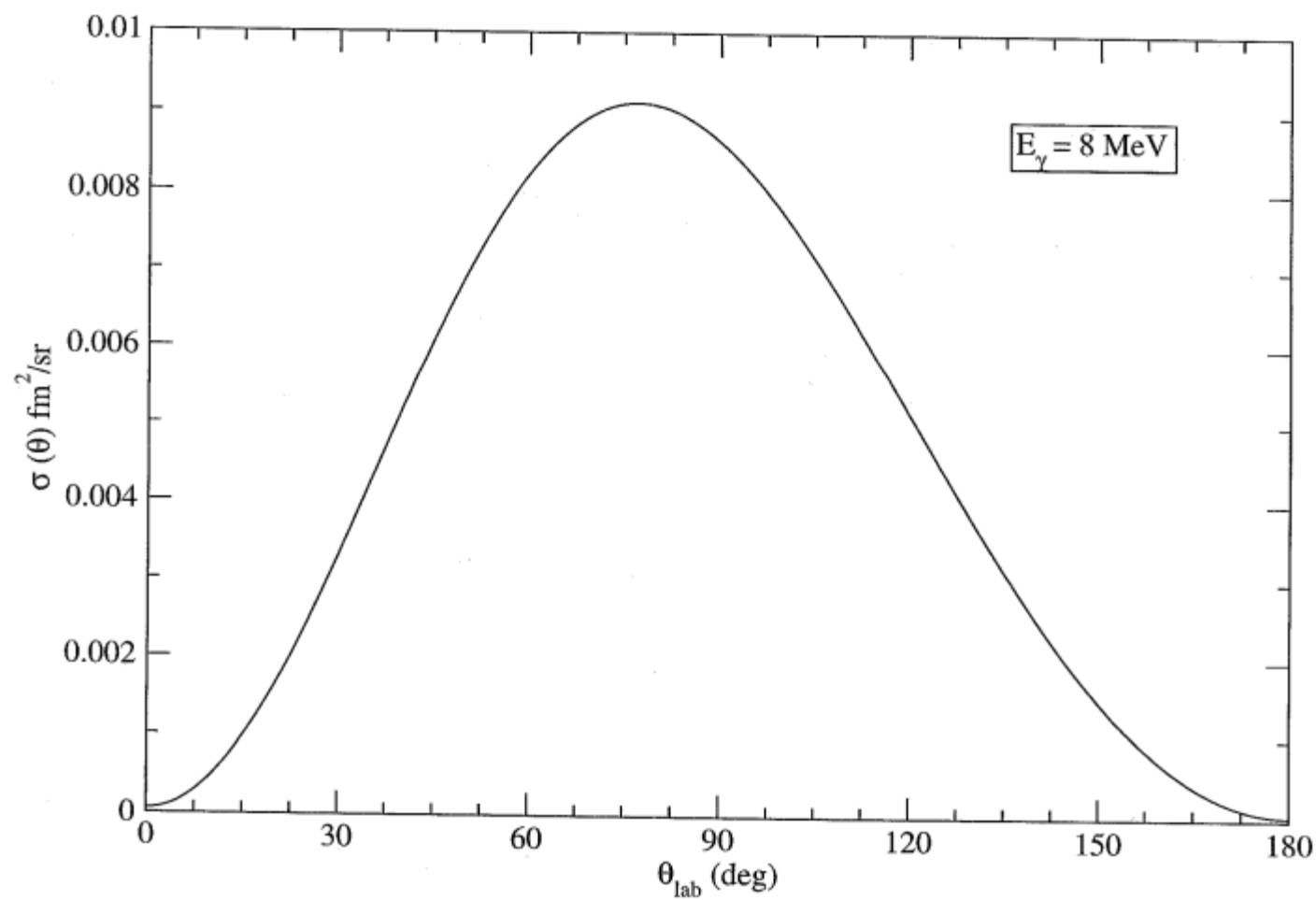
300 psi Xe & 450 psi ^3He at 12.78 MeV

294 psi Xe & 442 psi ^3He at 14, 15, 16 MeV

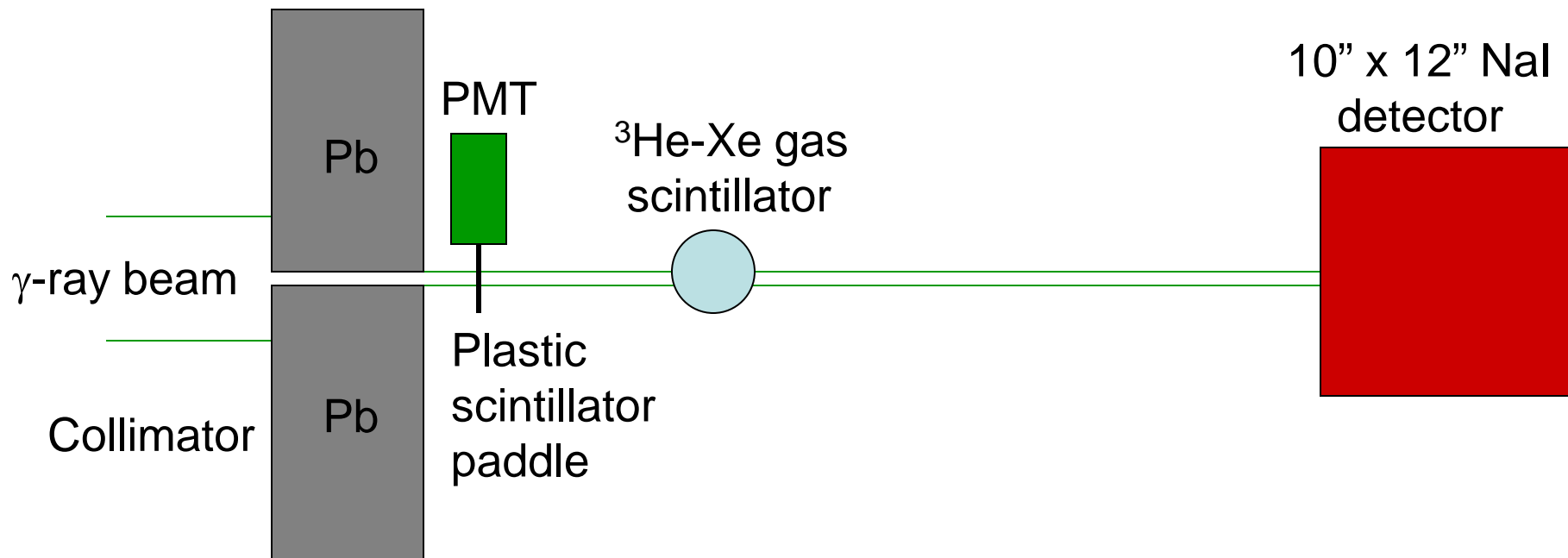


Edge Effects: Range of protons <1 cm





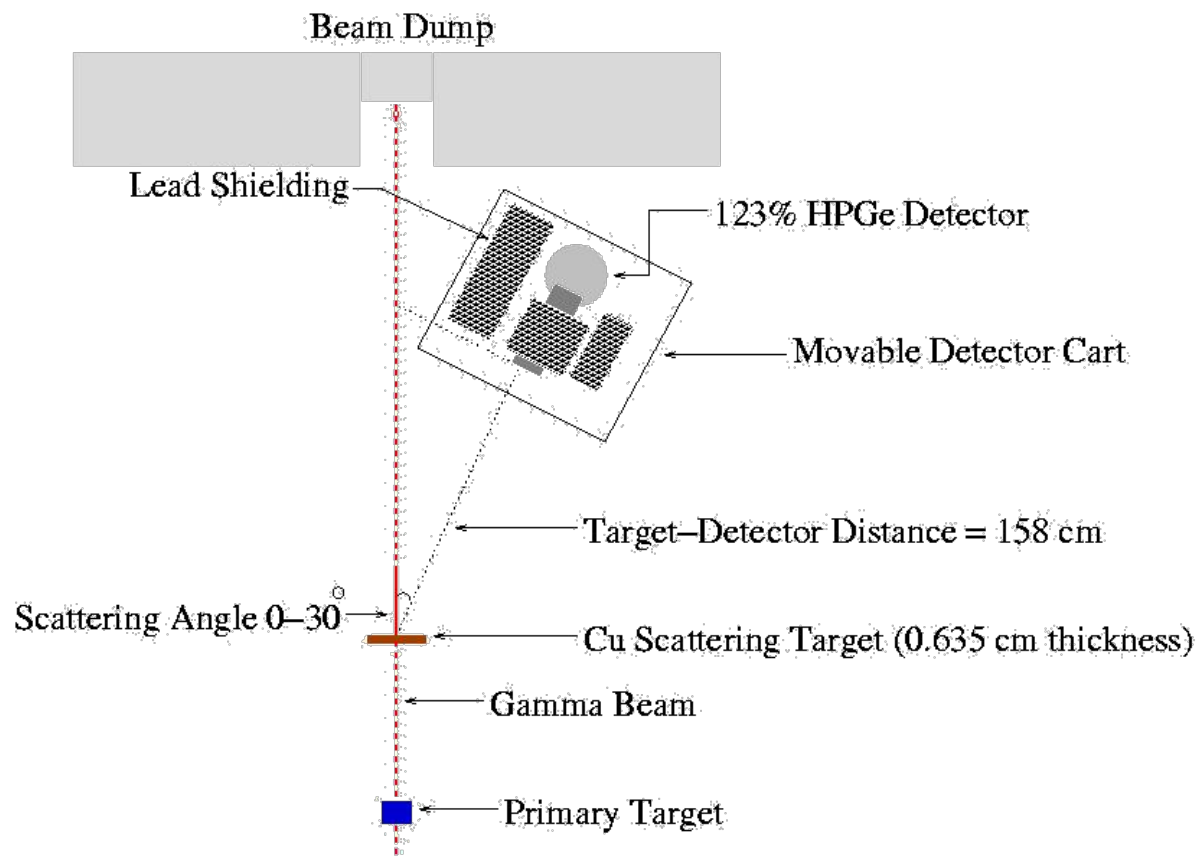
Photon Flux Determination



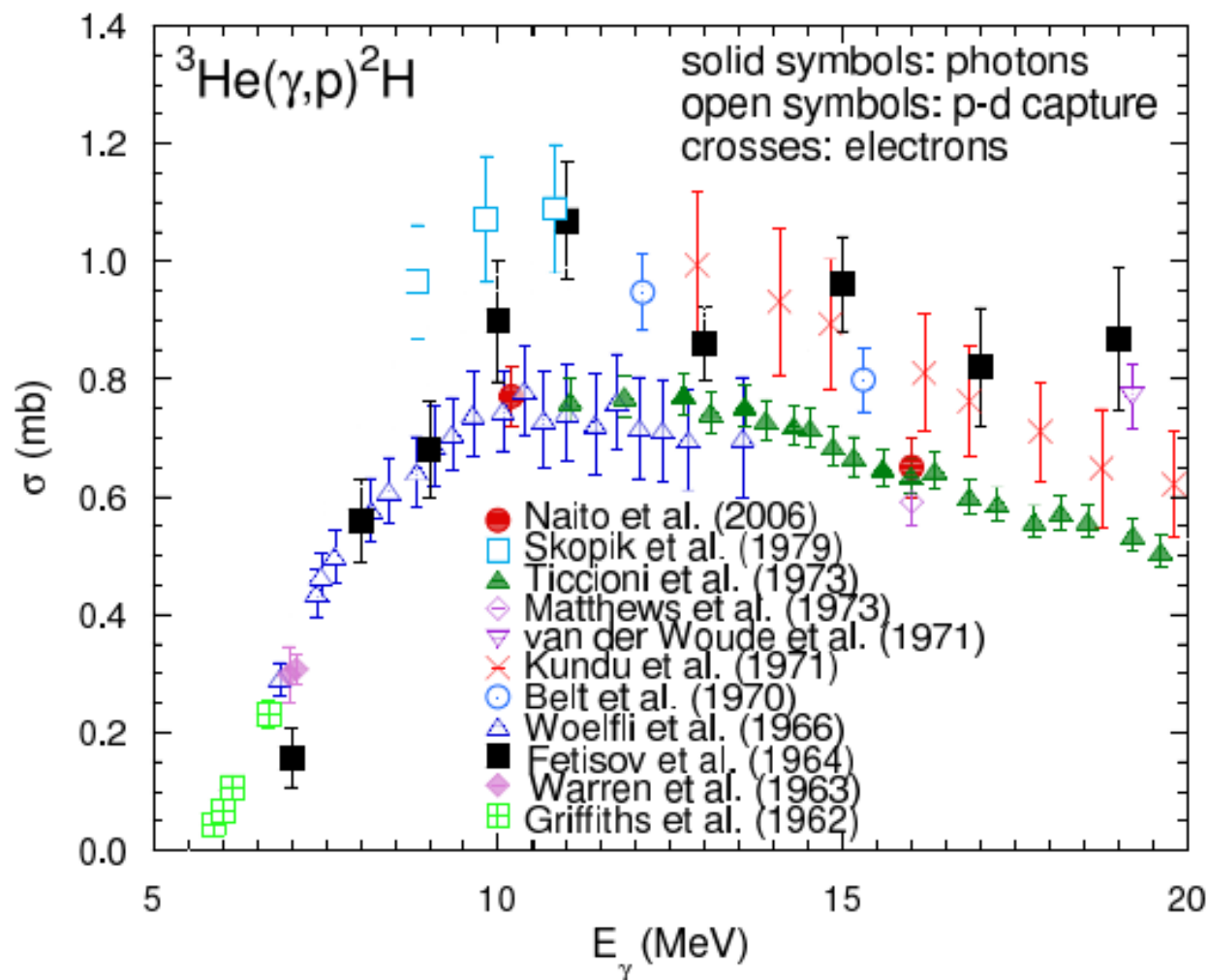
- 1) Move ${}^3\text{He} - \text{Xe}$ gas scintillator out of the photon beam
- 2) Reduce γ -ray flux to a few kHz rate
- 3) Move NaI scintillator of known efficiency into photon beam
- 4) Take data to determine ratio of Plastic Scintillator Paddle and NaI detector counts
- 5) Move NaI detector out of the photon beam
- 6) Move ${}^3\text{He} - \text{Xe}$ gas scintillator into the photon beam
- 7) Increase γ -ray flux to about 1 MHz
- 8) Take ${}^3\text{He}(\gamma, \text{pd})$ data
- 9) Use Plastic Scintillator Paddle yield and 4) to determine γ -rays used in 8)

Statistical Uncertainty: <1%
Systematic Uncertainty: 4% (NaI detector efficiency)

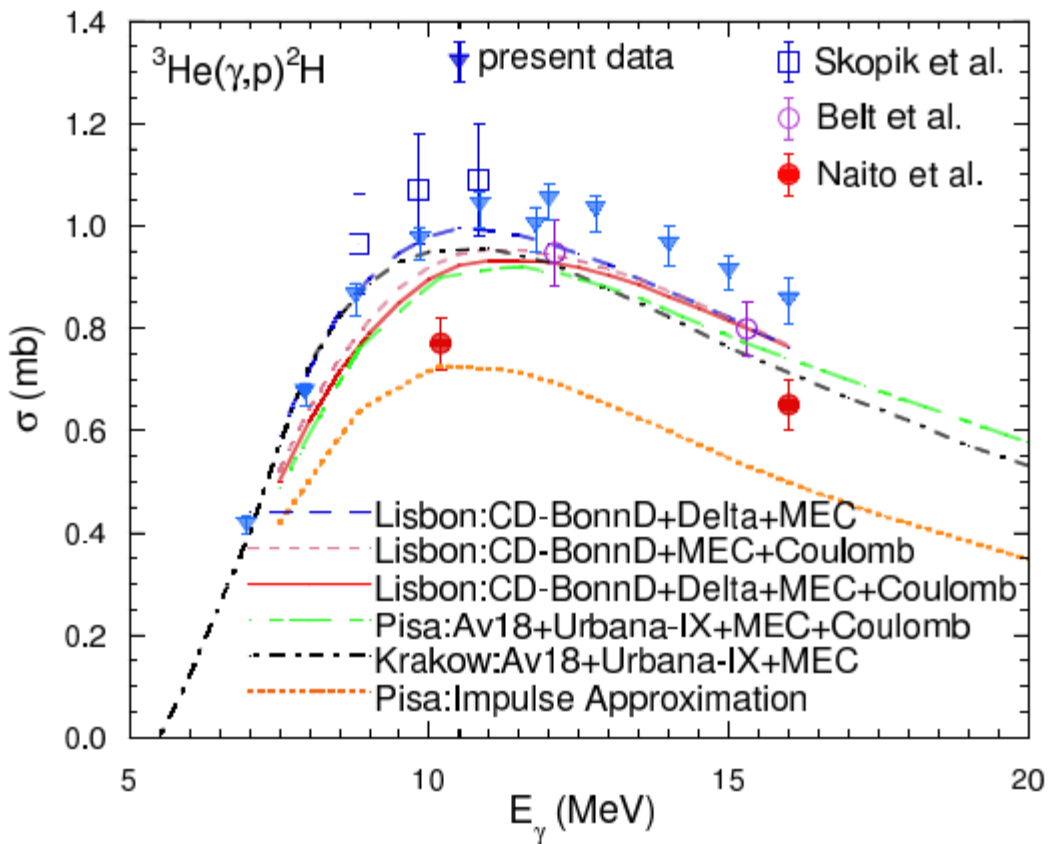
Check on γ -ray flux via Compton scattering from a Cu plate into an off-axis HPGe detector at energies below 10 MeV



Check on γ -ray flux determination via activation: $^{197}\text{Au}(\gamma,\text{n})^{196}\text{Au}$ between 12 and 16 MeV



$^3\text{He}(\gamma, \text{p})^2\text{H}$



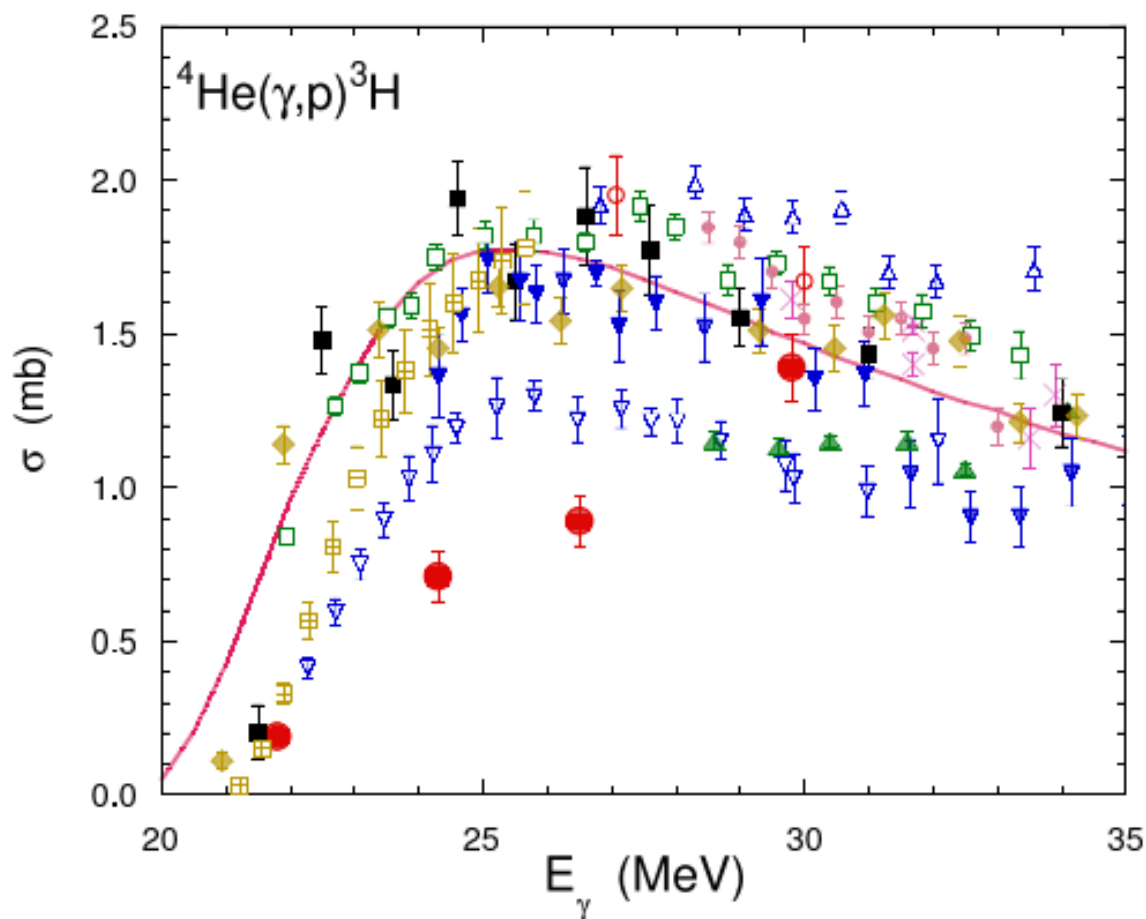
ukup

Electromagnetic interactions of 4N systems

$\gamma + {}^4\text{He} = {}^3\text{H} + p$	$Q = -19.81 \text{ MeV}$
$\gamma + {}^4\text{He} = {}^3\text{He} + n$	$Q = -20.58 \text{ MeV}$
$\gamma + {}^4\text{He} = d + d$	$Q = -23.85 \text{ MeV}$ (isospin forbidden)
$\gamma + {}^4\text{He} = d + n + p$	$Q = -26.07 \text{ MeV}$
$\gamma + {}^4\text{He} = n + p + n + p$	$Q = -28.30 \text{ MeV}$

${}^4\text{He}(\gamma, \text{pt})$

Trento Group: G. Orlandini, W. Leidemann, S. Quaglioni, N. Barnea, V.D. Efros,
Lorentz integral transform method, final-state interaction and Coulomb included, MTI-III



“New constraints on radiative decay of long lived particles in big bang nucleosynthesis with new ${}^4\text{He}$ photodisintegration data” by M. Kusakabe et al., Phys. Rev. D 79, 123513 (2009)

Now using ${}^4\text{He}$ -Xe gas scintillators

Photon Energy (MeV)	Xe (psi)	${}^4\text{He}$ (psi)	Proton Energies (MeV)
22.0	50	700	1.3 - 1.9
22.5	50	700	
23.0	150	605	1.9 – 2.8
23.5	150	605	
24.0	150	605	2.6 – 3.6
24.5	200	400	
25.0	200	400	3.3 – 4.4
25.5	200	400	
26.0	250	500	3.9 – 5.2
26.5	250	500	
27.0	250	500	4.6 – 6.1
27.5	250	500	
28.0	350	400	5.3 – 6.9
28.5	350	400	
29.0	350	400	6.0 – 7.7
29.5	350	400	

Photon-induced reaction thresholds (in MeV) on xenon isotopes

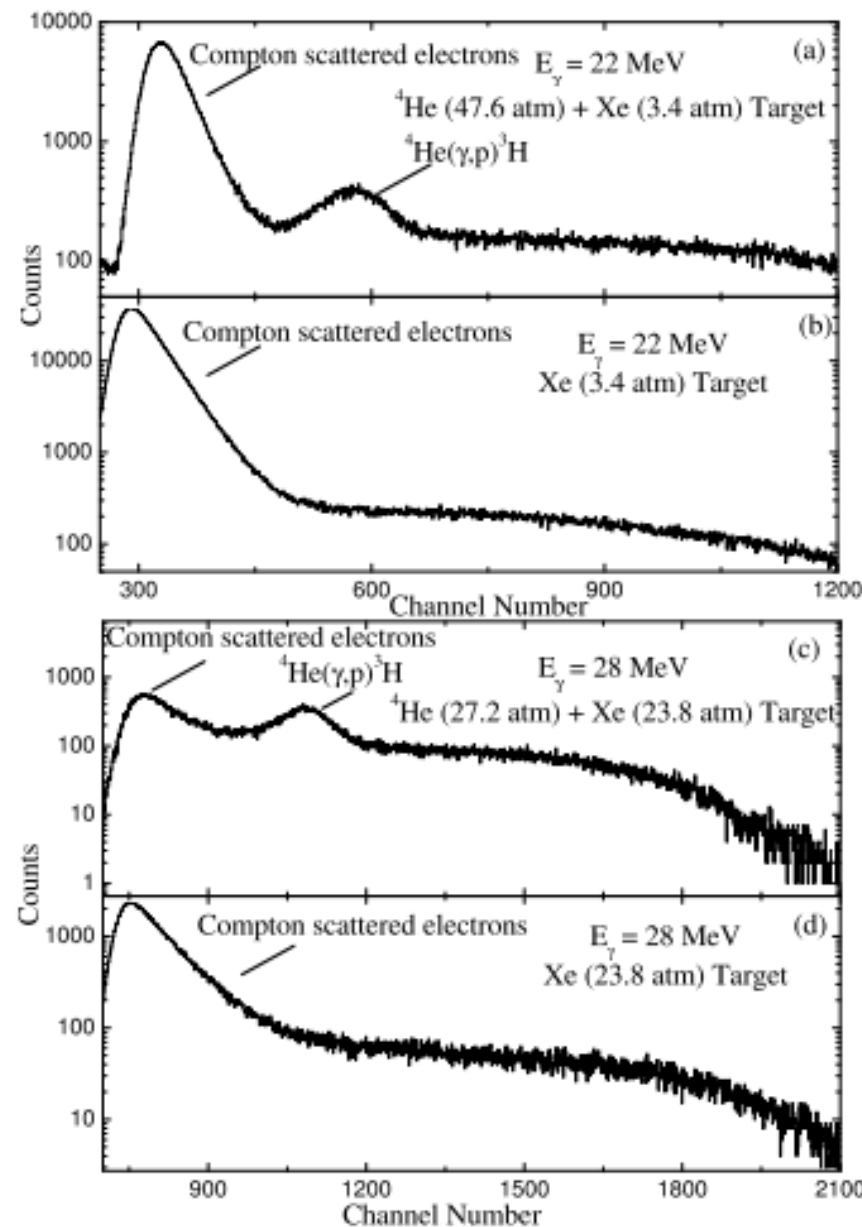
Isotope	Nat. Abundance (%)	(γ,p)	(γ,α)	(γ,n)	$(\gamma,2n)$	$(\gamma,n\alpha)$
128	1.92	8.17	1.77	9.61	16.84	11.19
129	26.44	8.25	2.09	6.91	16.52	8.68
130	4.08	8.67	2.24	9.26	16.16	11.35
131	21.18	8.82	2.55	6.61	15.87	8.85
132	26.89	9.12	2.71	8.93	15.54	11.48
134	10.44	9.55	3.20	8.54	14.99	11.62
136	8.87	9.93	3.66	7.99	14.44	11.73

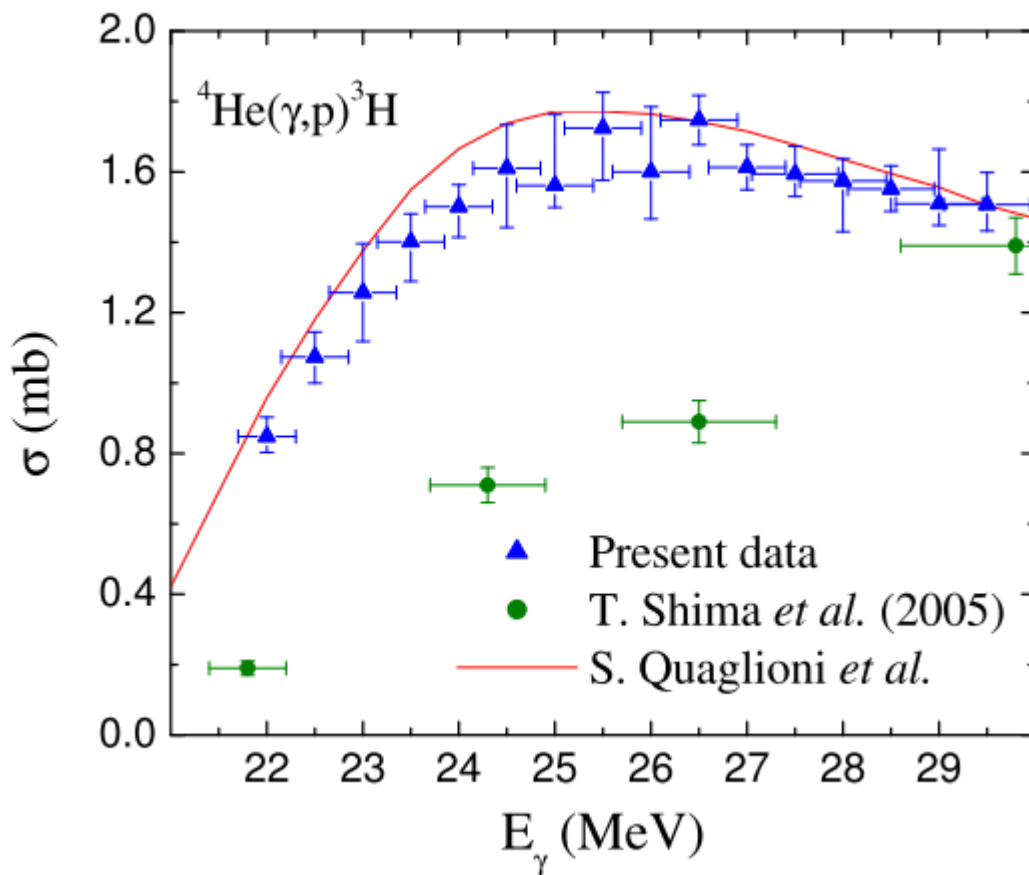
Photon-induced reaction thresholds (in MeV) on magnesium isotopes

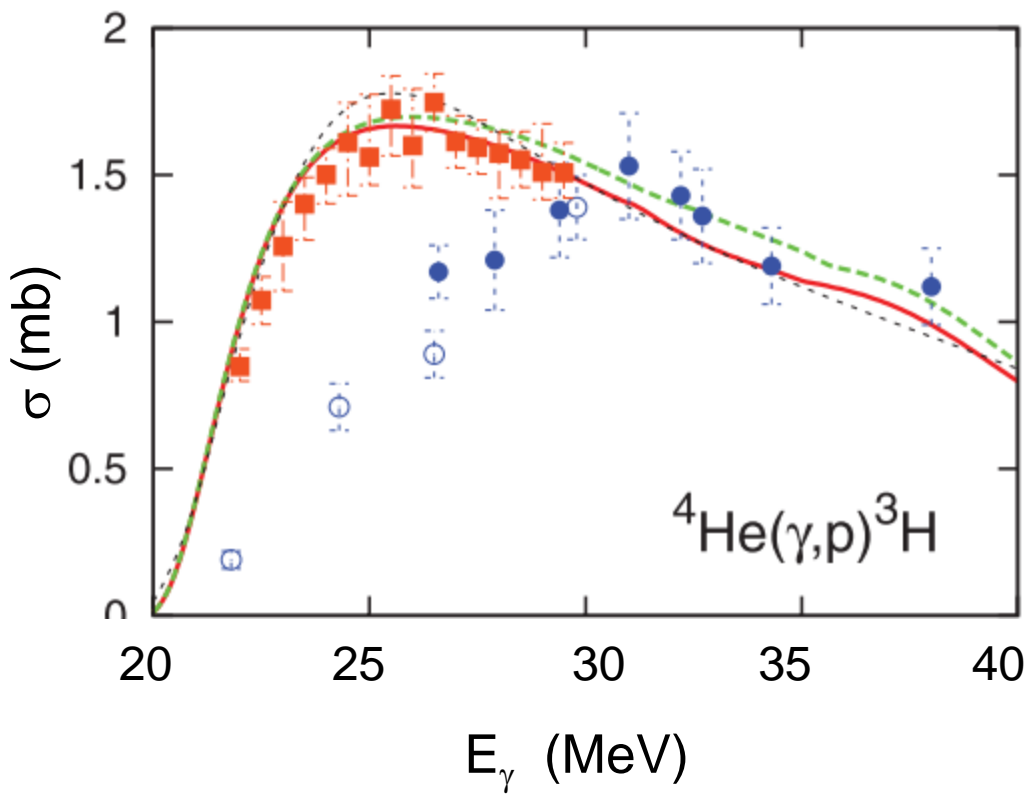
Isotope	Nat. Abundance (%)	(γ,p)	(γ,α)	(γ,n)	$(\gamma,2n)$	$(\gamma,n\alpha)$
24	78.99	11.69	9.31	16.53		
25	10.00	12.06	9.89	7.33		
26	11.01	14.15	10.61	11.09		

Photon-induced reaction thresholds (in MeV) on oxygen isotopes

Isotope	Nat. Abundance (%)	(γ ,p)	(γ , α)	(γ ,n)	(γ ,2n)	(γ ,n α)
16	99.762	12.13	7.16	15.67		
17	0.038	13.78	6.36	4.14		
18	0.200	15.94	6.23	8.05		



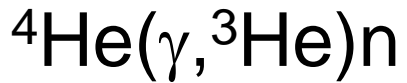




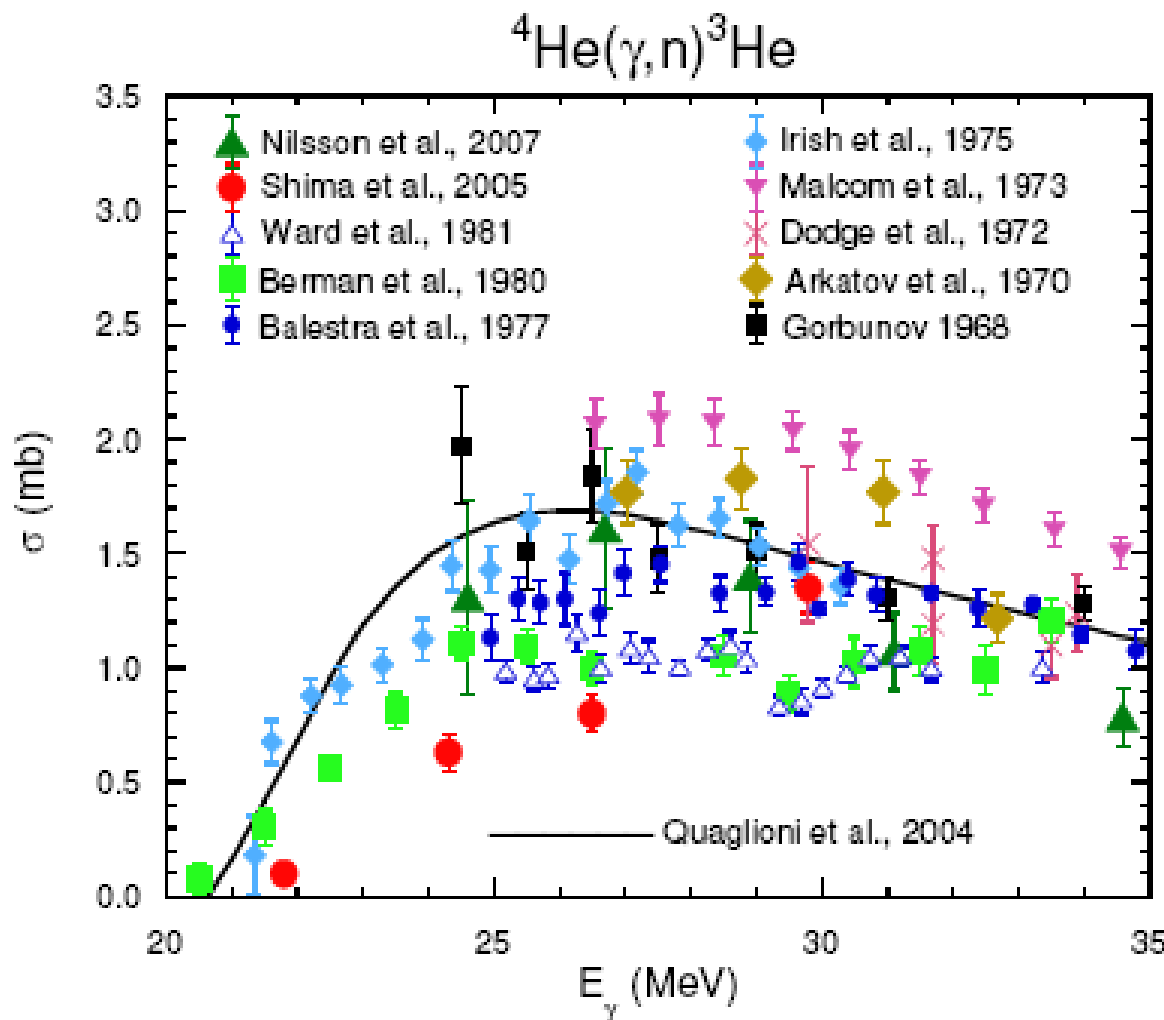
Circles: old data of Shima et al.
Dots: new data of Shima et al.

W. Horiuchi
Y. Suzuki
K. Arai

Solid: AV8'
Dashed: G3RS + 3NF (Tamagaki)
Dotted: LIT with Malfliet Tjon

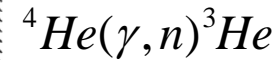
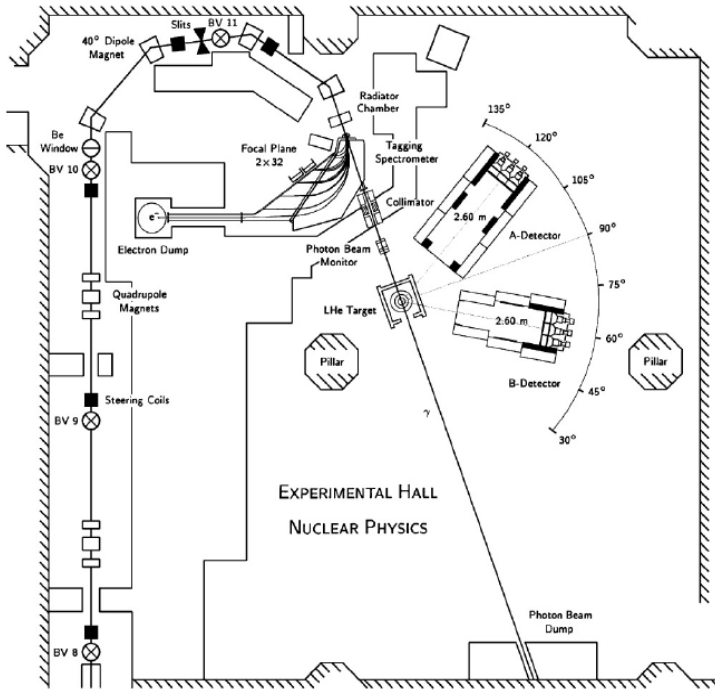


Trento Group: G. Orlandini, W. Leidemann, S. Quaglioni, N. Barnea, V.D. Efros,
Lorentz integral transform method, final-state interaction and Coulomb included, MTI-III



MAX – lab at Lund, Sweden

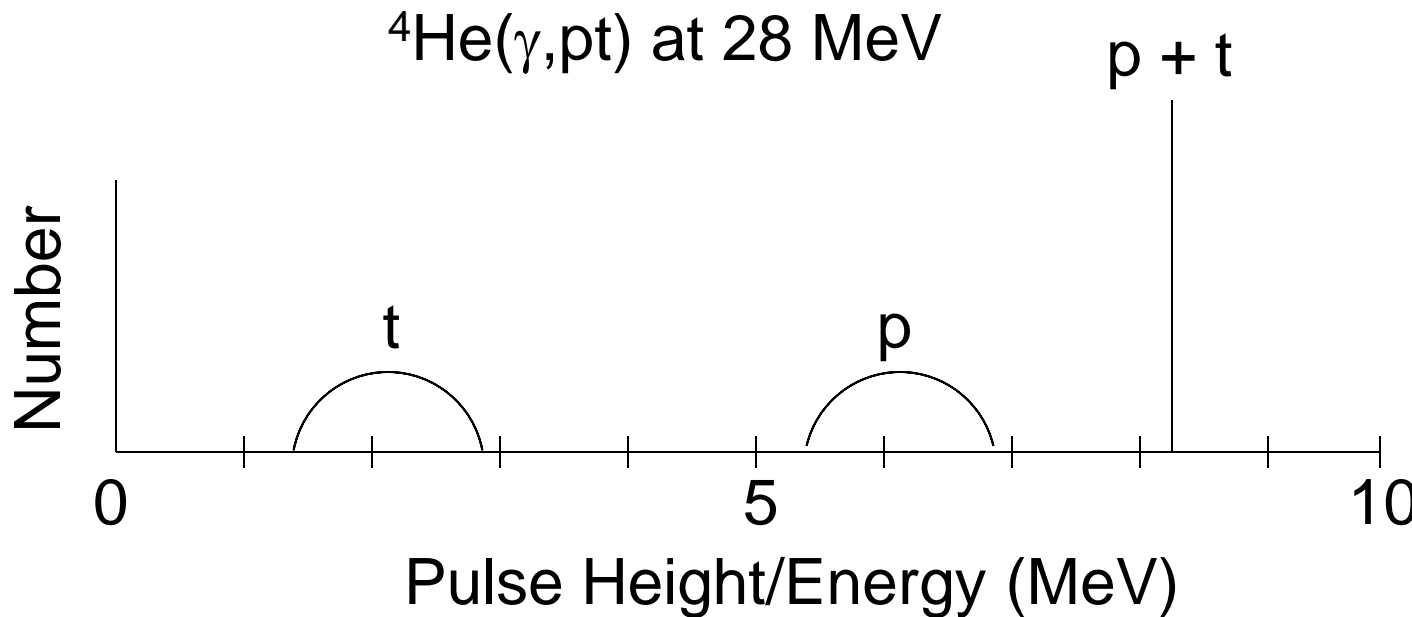
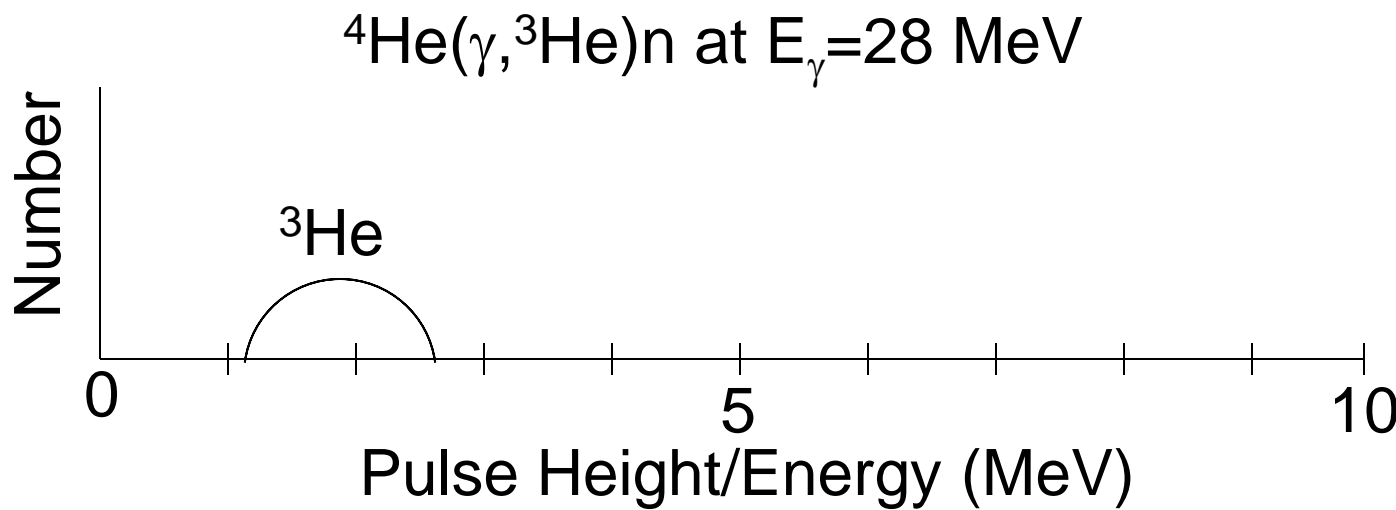
Bremsstrahlung
tagging technique

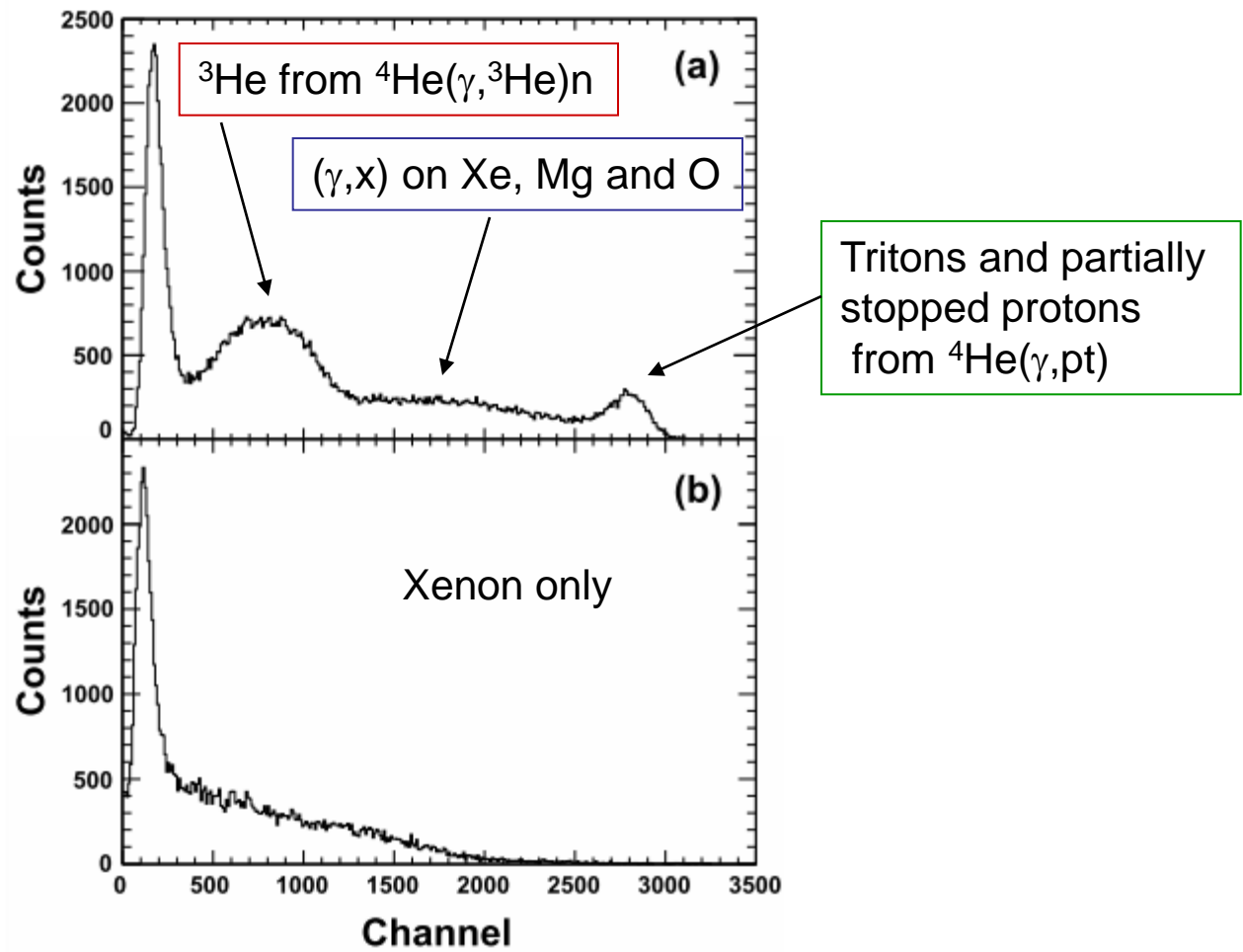


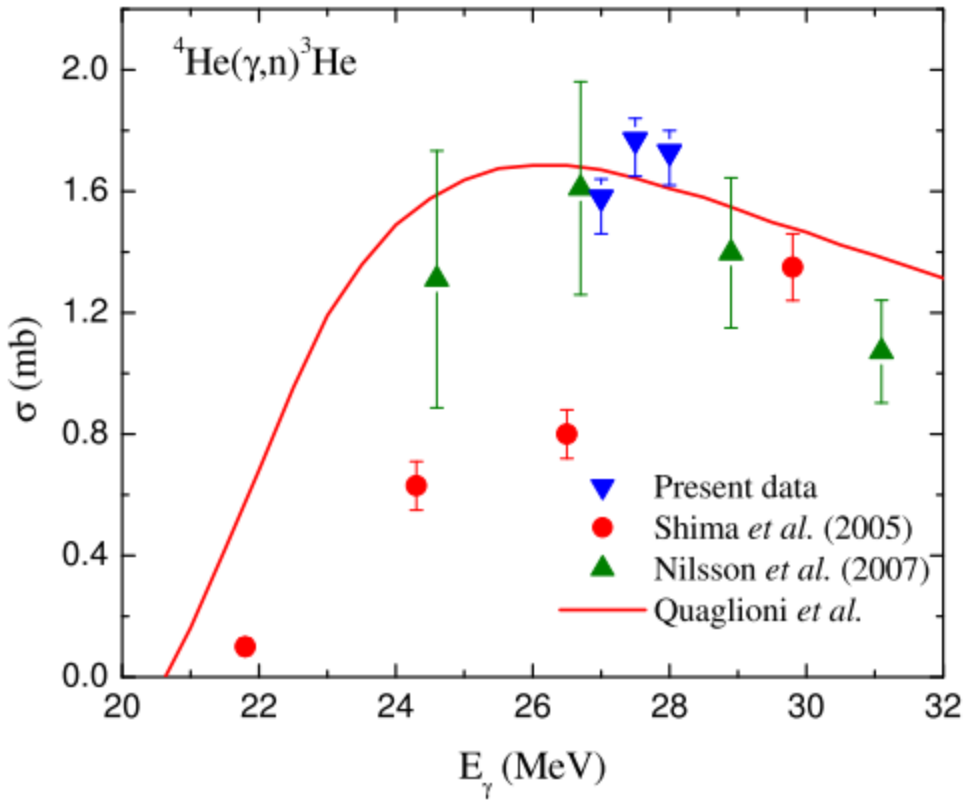
Neutron
detectors

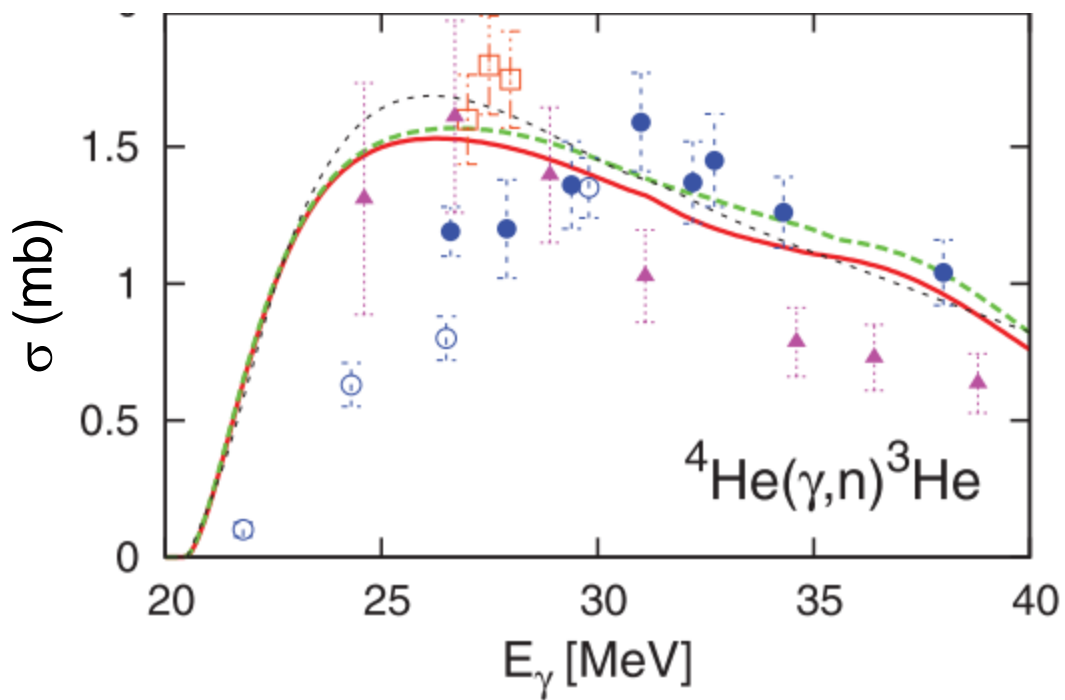
~300 keV γ -ray energy width

10^5 γ rays per second









Circles: old data of Shima et al.
 Dots: new data of Shima et al.
 Triangles: Nilsson et al.

W. Horiuchi
 Y. Suzuki
 K. Arai

Solid: AV8' = 3NF
 Dashed: G3RS + 3NF
 Dotted: LIT Malfliet-Tjon

What's next ?



PHYSICAL REVIEW C 85, 064003 (2012)

Di-neutron and the three-nucleon continuum observables

H. Witała

M. Smoluchowski Institute of Physics, Jagiellonian University, PL-30059 Kraków, Poland

W. Glöckle

Institut für Theoretische Physik II, Ruhr-Universität Bochum, D-44780 Bochum, Germany

(Received 24 April 2012; published 25 June 2012)

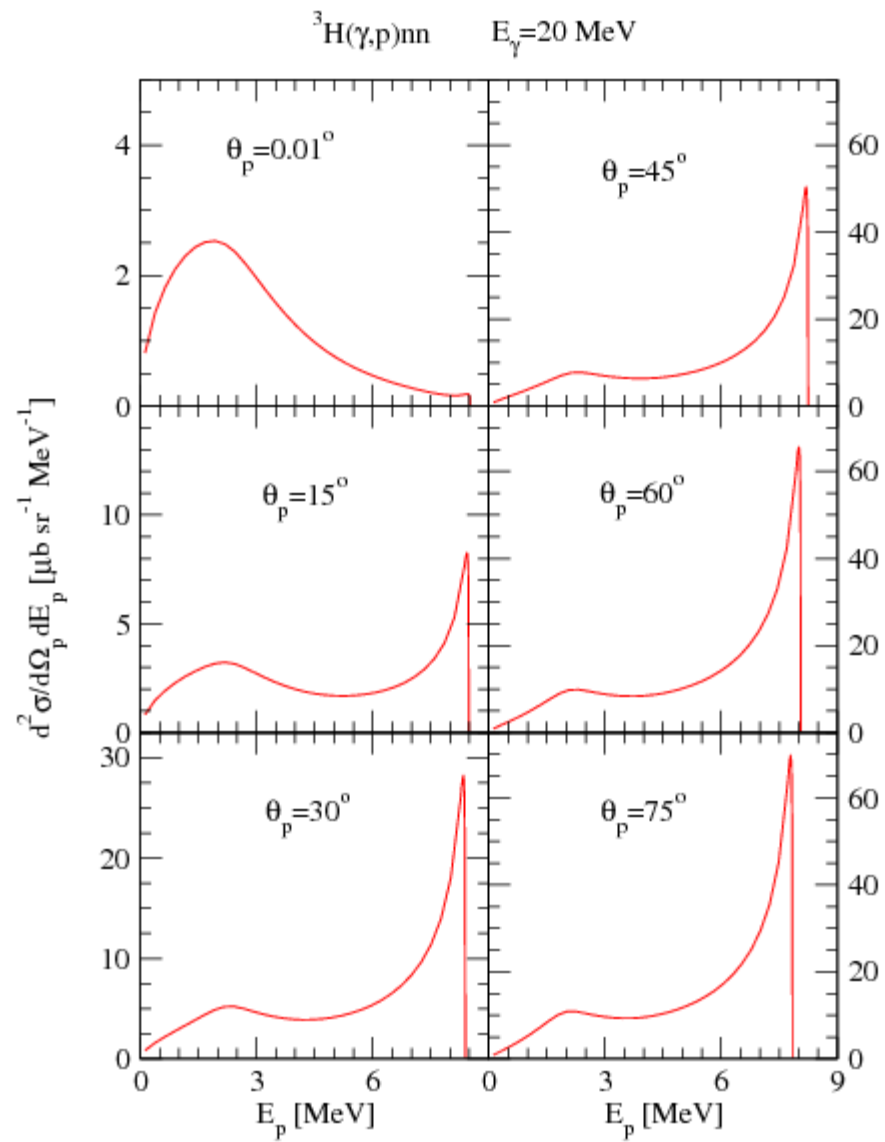
We investigate how strongly a hypothetical 1S_0 bound state of two neutrons would affect observables in neutron-deuteron reactions. To that aim we extend our momentum-space scheme of solving the three-nucleon Faddeev equations and incorporate in addition to the deuteron also a 1S_0 di-neutron bound state. We discuss effects induced by a di-neutron on the angular distributions of the neutron-deuteron elastic scattering and deuteron breakup cross sections. A comparison to the available data for the neutron-deuteron total cross section and elastic scattering angular distributions cannot decisively exclude the possibility that two neutrons can form a 1S_0 bound state. However, strong modifications of the final-state-interaction peaks in the neutron-deuteron breakup reaction seem to disallow the existence of a di-neutron.

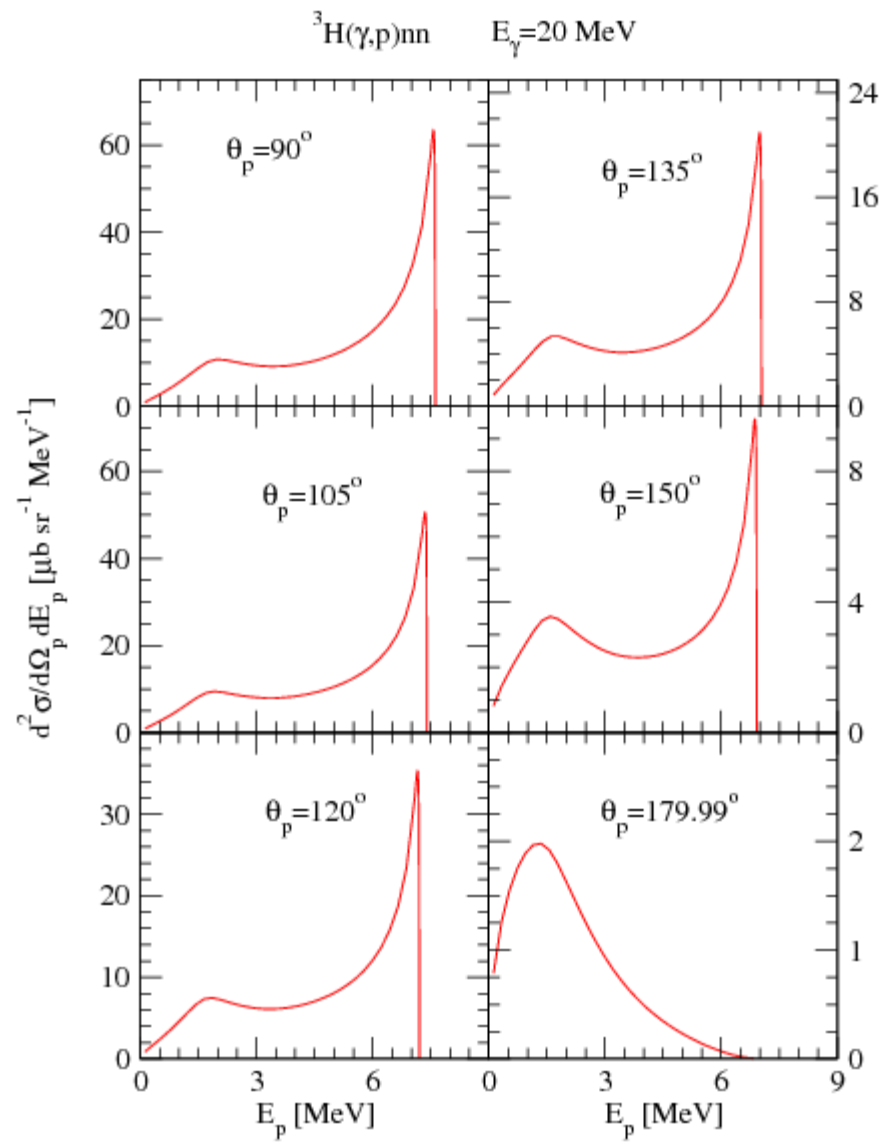
DOI: [10.1103/PhysRevC.85.064003](https://doi.org/10.1103/PhysRevC.85.064003)

PACS number(s): 21.45.Bc, 25.10.+s, 25.40.Dn

TABLE I. The di-neutron binding energy ϵ_{nn} , the nn scattering length a_{nn} , and the effective range parameter r_{eff} for different factors λ by which the nn 1S_0 component of the CD Bonn potential was multiplied.

λ	ϵ_{nn} [MeV]	a_{nn} [fm]	r_{eff} [fm]
0.9	—	-8.25	3.12
1.0	—	-18.80	2.82
1.19	-0.099	+21.69	2.39
1.21	-0.144	+18.22	2.35
1.3	-0.441	+10.95	2.20
1.4	-0.939	+7.87	2.07





Changing Topics:

$A_y(\theta)$ in ${}^3\text{He}(n,n){}^3\text{He}$
and Comparison to ${}^3\text{He}(p,p){}^3\text{He}$
at Low Energies

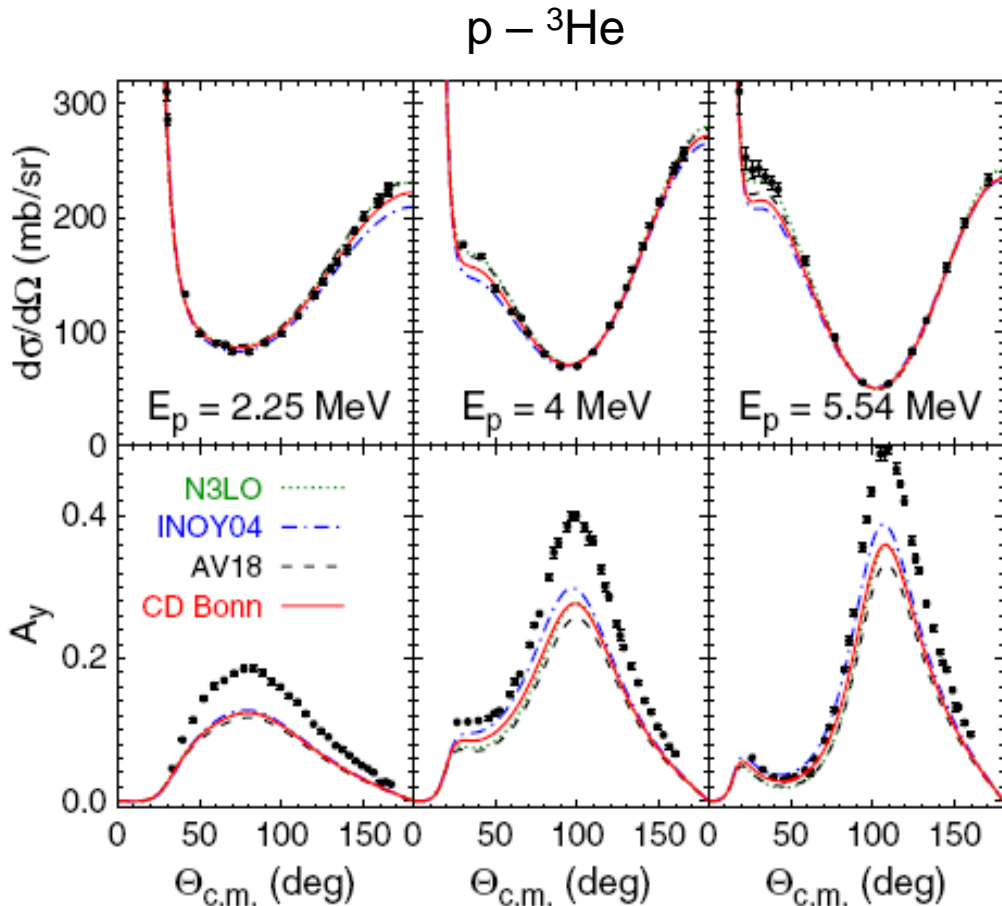
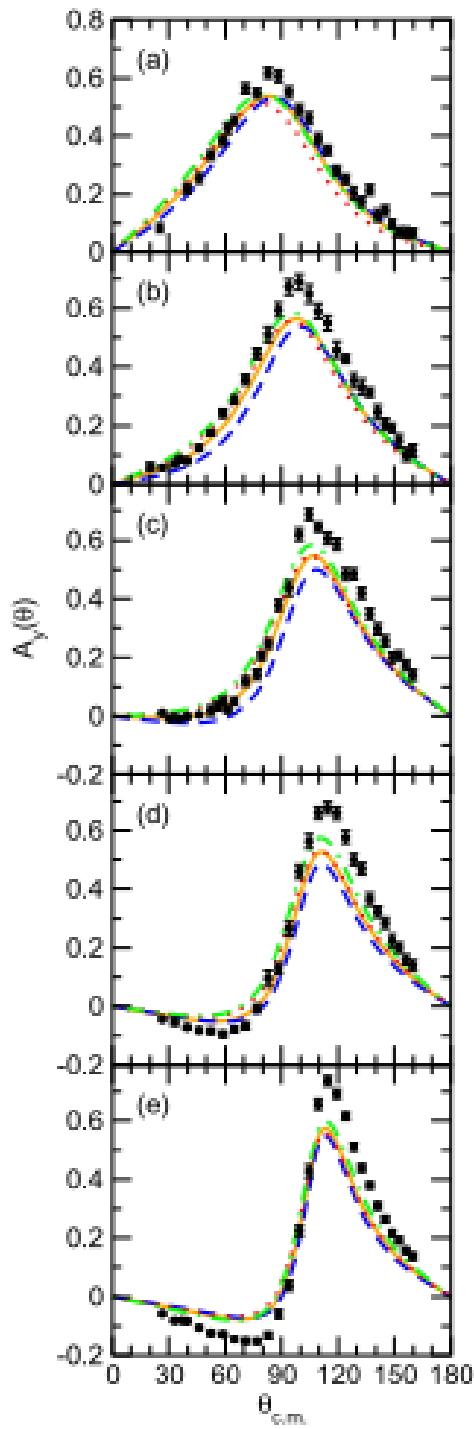


FIG. 2 (color online). The differential cross section and proton analyzing power A_y at 2.25, 4.0, and 5.54 MeV proton lab energy. Results including the Coulomb interaction obtained with potentials CD Bonn (solid curves), AV18 (dashed curves), INOY04 (dashed-dotted curves), and N3LO (dotted curves) are compared. The data are from Refs. [22,32,33].



$E_n = 1.60 \text{ MeV}$

$E_n = 2.26 \text{ MeV}$

$E_n = 3.14 \text{ MeV}$

$E_n = 4.05 \text{ MeV}$

$E_n = 5.54 \text{ MeV}$

Data: ${}^3\text{He}(n,n){}^3\text{He}$
J.H. Esterline

Dashed blue: AV18

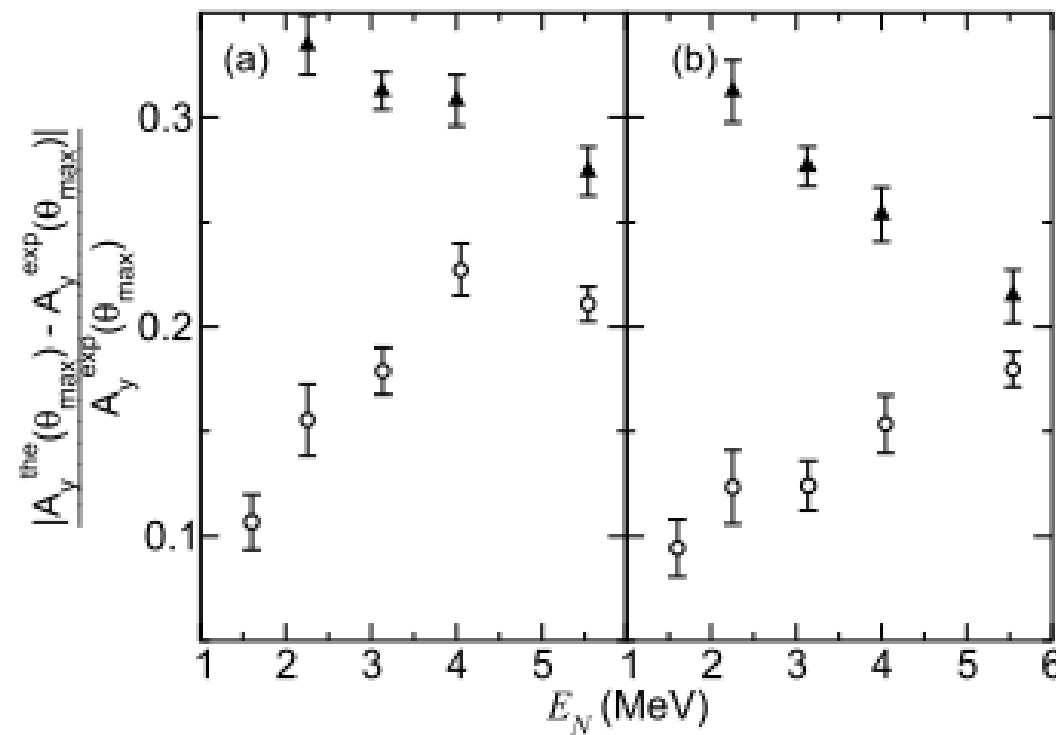
Solid orange: CD-Bonn

Dotted red: CD-Bonn + Δ

Dashed-dotted green: INOY04

Calculations:
A. Deltuva & A. Fonseca

Triangles: ${}^3\text{He}(\text{p},\text{p}){}^3\text{He}$
Circles: ${}^3\text{He}(\text{n},\text{n}){}^3\text{He}$



CD-Bonn INOY04 (Doleschall)

A. Deltuva (Lisbon)

Acknowledgments

J.H. Esterline
M.W. Ahmed
A.S. Crowell
H.J. Karwowski
J.H. Kelley
R. Pywell
R. Raut
G. Rusev
S.C. Stave
A.P. Tonchev

and to all the theoreticians I had the pleasure to interact with.